The American Journal of Pathology, Vol. 175, No. 3, September 2009

DOI: 10.2353/ajpath.2009.090125

Neurobiology

Prion Protein with an Insertional Mutation Accumulates on Axonal and Dendritic Plasmalemma and Is Associated with Distinctive Ultrastructural Changes

Martin Jeffrey,* Caroline Goodsir,* Gillian McGovern,* Sami J. Barmada,† Andrea Z. Medrano,† and David A. Harris†

From the Veterinary Laboratories Agency, Lasswade Laboratory, Pentlands Science Park, Bush Loan, Penicuik, Midlothian, Scotland; and the Department of Cell Biology and Physiology,† Washington University School of Medicine, St. Louis, Missouri*

Prion diseases are fatal neurological diseases characterized by central nervous system deposition of abnormal forms of a membrane glycoprotein designated PrP (prion protein). Tg(*PG14*) transgenic mice express PrP that harbor a nine-octapeptide insertional mutation homologous to one described in a familial prion disease of humans. Tg(*PG14*) mice spontaneously develop a fatal neurological illness accompanied by massive apoptosis of cerebellar granule neurons and accumulation of an aggregated and weakly protease-resistant form of PrP that is not infectious. Previous light microscopic analyses of these mice left open questions regarding the subcellular distribution of the mutant protein and the nature of the neuropathological lesions produced. To address these questions, we undertook an immunogold electron microscopic study of Tg(*PG14*) mice. We found that mutant PrP is localized primarily on the plasma membrane of dendrites and unmyelinated axons in the hippocampus and cerebellum, with little labeling of either neuronal cell bodies or intracellular organelles. PrP deposits were shown to be associated with degenerative changes in dendritic structure. We also describe for the first time marked pathology in myelinated axons, and alterations in the axon/oligodendrocyte interface. Taken together, our results suggest cellular mechanisms by which mutant PrPs produce pathology. In addition, they highlight distinctions between familial and infectious prion disorders at the ultrastructural level that correlate with differences in cellular trafficking of the disease-associated PrP forms. ***(Am J Pathol 2009, 175:1208–1217; DOI: 10.2353/ajpath.2009.090125)***

Transmissible spongiform encephalopathies, or prion diseases, are fatal neurological disorders of humans and animals that occur in sporadic, contagious and familial forms.[1] A key molecular event in all prion diseases is the conversion of a normal cell-surface sialoglycoprotein (PrP^{C}) into a conformationally altered isoform (PrP^{Sc}) that is enriched in β-sheet structure.[2] PrP^{Sc}, which is typically identified by its increased resistance to protease digestion, has been claimed to be infectious in the absence of nucleic acid.[3] However, there is evidence that some pathogenic forms of PrP are not infectious, and that some may be protease sensitive.[4–6]

Immunohistochemical methods have been used to visualize disease-specific accumulations of PrP (PrP^{d}), encompassing both protease-resistant and protease-sensitive forms, in tissues of infected animals.[7] These studies have shown that accumulations of PrP^{d} occur predominantly on the perikaryonal and dendritic plasma membranes of neurons, and within lysosomes.[8–10] Such PrP^{d} accumulations specifically co-localize with several kinds of cellular pathology, including abnormal endocytic

Supported by UK government (Defra) grant Se 1940, and in Dr. Harris' laboratory (NS040975) by the National Institutes of Health. S.J.B. was supported by the Medical Scientist Training Program at Washington University (NIH grant T32GM07200).

Accepted for publication May 19, 2009.

Current address of S.J.B., Department of Neurology, UCSF Medical Center, 505 Parnassus Avenue, Box 0114, San Francisco, CA.

Address reprint requests to Martin Jeffrey, Veterinary Laboratories Agency, Lasswade Laboratory, Pentlands Science Park, Bush Loan, Penicuik, Midlothian, Scotland EH26 0PZ. E-mail: m.jeffrey@vla.defra.gsi.gov.uk; or David A. Harris, Department of Biochemistry, Boston University School of Medicine, 72 East Concord street, K225, Boston, MA 02118. E-mail: daharris@bu.edu.

Table 1. Transgenic Mice Examined by Light and Electron Microscopy

Genotype*	Tg lines and no. of mice	Age (days)	Disease status
$PG14^{+/-}$	A2 ($n = 2$); A3 ($n = 2$)	246 to 264	Mild signs
$PG14^{+/-}$	A2 ($n = 2$); A3 ($n = 3$)	361 to 394	Terminally ill
$WT^{+/+}$	E1 ($n = 5$)	195 to 384	Healthy

*For a description of these transgenic lines, see Chiesa et al.[12]

structures, microfolding of the plasma membrane, and excess lysosomes.[9] In several murine scrapie models (eg, ME7), there is also conspicuous synaptic loss (not co-localized with PrP^d), as well as marked degeneration of axons.[11]

Tg(*PG14*) mice express the murine homologue of PrP carrying a nine-octapeptide insertional mutation described in human patients with an inherited prion disease.[12] These mice spontaneously develop a fatal, ataxic, neurological illness, and they accumulate in their brains an insoluble and weakly protease-resistant form of the mutant protein that shares certain biochemical similarities with abnormal PrP derived from infectious prion sources.[13] However, PrP from Tg(*PG14*) mice is not infectious in transmission experiments or in cell-free amplification reactions.[5,13] Tg(*PG14*) mice therefore provide an ideal model for investigation of PrP pathogenic mechanisms independent of mechanisms of prion infectivity.

The neuropathological features of Tg(*PG14*) mice have been previously characterized by light microscopy.[12,14] These animals display a marked cerebellar cortical atrophy associated with apoptosis of granule neurons and thinning of the synapse-rich molecular layer. Immunohistochemistry shows accumulation of *PG14* PrP in neuropil regions throughout the brain as diffuse, non-amyloid deposits previously characterized as "synaptic-like." In addition, prominent intra-axonal deposits of the mutant protein have been described in Tg(*PG14-EGFP*) mice that express *PG14* PrP fused to enhanced green fluorescent protein.[15]

The Tg(*PG14*) mouse represents a model of inherited prion disease in which the neuropathology induced by a mutant prion protein can be studied in detail. However, previous light microscopic analyses of Tg(*PG14*) brains left open several important questions. Most importantly, what is the subcellular distribution of *PG14* PrP deposits, and are such deposits associated with degenerative morphological changes in neurons or other cell types? To address this question, and to compare the lesions associated with *PG14* PrP to those associated with PrP^d accumulations in infectious prion diseases, we have undertaken an immunogold electron microscopic analysis of the brains of Tg(*PG14*) mice. Our results significantly extend previous understanding of the neuropathology of Tg(*PG14*) mice, providing insight into cellular mechanisms operative in familial prion diseases and how these compare to the processes underlying infectious prion diseases.

Materials and Methods

Animals

Tg($PG14^{+/-}$)/$Prn\text{-}p^{O/O}$ mice (A2 and A3 lines) and Tg($WT^{+/+}$)/$Prn\text{-}p^{O/O}$ mice (E1 line) have been described previously.[12] Nine hemizygous Tg(*PG14*) mice of A2 and A3 lines and five Tg(*WT*) were analyzed in this study (Table 1).

Tissue Preparation

Mice were perfusion-fixed with 4% paraformaldehyde and 0.1% glutaraldehyde, and their brains were sagittally sectioned in the midline. Half-brains were fixed and embedded in paraffin wax for preliminary light microscopic analysis to confirm the neuroanatomic distribution of pathology and *PG14* PrP accumulation. From the contralateral half-brain, multiple 1-mm^3 tissue blocks were sampled from the hippocampus and cerebellum, postfixed in osmium tetroxide and embedded in araldite resin.

Light Microscopic Immunohistochemical Procedures

Light microscopic immunohistochemistry was performed using both paraffin wax- and resin-embedded blocks. Tissue sections, 3 μm thick, were cut from paraffin wax blocks on a microtome, mounted on treated glass slides (Superfrost Plus; Menzel-Glaser, Germany), and dried overnight at 60°C. The sections were de-waxed and hydrated, and then subjected to antigen-retrieval procedures. Sections were immersed in 98% formic acid for 5 minutes, washed in running tap water for 5 minutes, and then immersed in 0.2% citrate buffer and autoclaved for 30 minutes at 121°C. The following blocking steps were then applied: 3% hydrogen peroxide in ethanol for 20 minutes to block endogenous peroxidase; 5% normal serum for 60 minutes followed by diluent (Vector MOM Kit: Vector Laboratories, Peterborough, UK) for 5 minutes to block endogenous mouse immunoglobulins. Immunolabeling was performed according to the avidin-biotin complex immunohistochemical staining method (Vector-Elite Kit ABC). The reaction product was visualized using 3-3′ diaminobenzidine.

Anti-PrP antibodies 1A8 (1:10,000 dilution) and R24 (1:4000 dilution) were used for light microscopy of paraffin-embedded sections. 1A8 is a polyclonal antibody raised in rabbits against ME7 murine scrapie that recognizes multiple domains of the PrP molecule.[16] A pre-

Table 2. Comparison of Selected Lesions in the Cerebellum of Tg(*PG14*) Mice and Two Murine Scrapie Models

Genotype	Age (days)	Neuronal apoptosis	Dendrite degeneration*	Glial-neuritic ensheathing*	Irregular neurite contours*	Dysregulation of axon-oligodendrocyte interface	Axonal inclusion	Acute terminal axon necrosis†
PG14$^{+/-}$	246 to 267	++	+	+	++	+	+	−
PG14$^{+/-}$	361 to 394	+++	++	++	++	+++	++	−
WT$^{+/+}$	195 to 384	−	−	−	−	−	+/−	−
ME7 scrapie in *C57BL*‡	Terminal	+	−	+++	+++	−	+	+++
263K scrapie in *Tg3/Prn-p*$^{0/0}$‡	Terminal	+	−	+++	+++	−	+/−	+++

−, Not detected; +/−, +, ++, +++, Single, few, several, or many examples present (see *Materials and Methods* for scoring details).
*Lesions which are colocalized with *PG14* PrP or PrP^{d}.
†Several forms of dendritic and axonal pathology are present in murine scrapie that are absent from Tg(*PG14*) mice. The table selects for comparison only one of these changes, an acute form of terminal axon degeneration.
‡Murine scrapie data are taken from.[11,20,21]

challenge serum from this rabbit was used as an antibody control. Monoclonal antibody R24 recognizes an epitope encompassing amino acid residues 22 to 40 within the flexible tail of PrP.[17] Similar staining results were obtained using antibodies 6H4[18] and 3F4,[19] (data not shown). Paraffin-embedded tissue sections were also labeled with an antibody against glial fibrillary acidic protein (DakoCytomation UK Ltd., Cambridgeshire, UK; 1:500 dilution) or with a monoclonal antibody recognizing phosphorylated 200-kDa and 70-kDa neurofilament subunits (DakoCytomation UK Ltd., 1:250 dilution).

Resin-embedded sections were stained for PrP using 1A8 antibody, which was the only one tested that produced satisfactory immunolabeling. One-micron thick resin sections were etched using sodium ethoxide, and pretreated with 98% formic acid for 10 minutes, followed by 6% hydrogen peroxide in water for 10 minutes. Normal serum was then applied for 60 minutes. The avidin-biotin complex immunohistochemical staining method using 1A8 antiserum (1:6000 dilution) was applied to sections, and reaction product was developed using 3-3′ diaminobenzidine. Selected blocks with appropriate immunostained areas were then taken for ultrastructural studies.

Electron Microscopic Immunohistochemical Procedures

For routine electron microscopy, areas were selected from 1-μm thick immunolabeled, resin-embedded sections; 65-nm sections were cut from selected blocks and counterstained with uranyl acetate and lead citrate.

For ultrastructural immunohistochemistry, serial 65-nm sections from selected blocks were placed on 600 mesh gold grids and etched in sodium periodate for 60 minutes. Endogenous peroxidase was blocked, and sections de-osmicated with 6% hydrogen peroxide in water for 10 minutes, followed by enhancement of antigen exposure with formic acid for 10 minutes. 1A8 antiserum or preimmune serum at a 1:500 dilution in incubation buffer was then applied for 15 hours. After rinsing extensively, sections were incubated with Auroprobe (Amersham Ltd., Amersham, UK) 1-nm colloidal gold diluted 1:50 in incubation buffer for 2 hours. Sections were then postfixed with 2.5% glutaraldehyde in phosphate buffered saline, and labeling enhanced with immunogold silver preparation for 4 minutes. Grids were counterstained with uranyl acetate and lead citrate. In addition to labeling for PrP, immunogold labeling for ubiquitin was also performed, as previously described.[9] Sections were viewed in a Jeol 1200 EX electron microscope.

The frequency of morphological lesions was scored on cerebellar grids from each mouse. Following initial examinations of both hippocampus and cerebellum, all lesions were listed and photographed. A pro-forma was created listing each lesion observed with a five-step scoring scale, as follows: −, not recorded; +/− single example encountered in whole grid; + present, on average, once in every 15 grid squares; ++ present, on average, once in every 5 grid squares; +++ present, on average, in most grid squares. Blind, coded grids form each cerebellum were scored using this pro-forma. Table 2 shows the average values for mildly symptomatic, terminal, and control Tg mice. Subjective estimations of lesion severity for two infectious scrapie models are included in Table 2 for comparison, but no formal quantitation was performed for these models in this study. However, these models have been characterized extensively in previously published studies.[11,20,21]

Results

Tg(*PG14*) mice hemizygous for the *PG14* transgene array develop ataxia beginning at ~240 days of age, and die at 370 to 450 days of age.[14] Tg(*WT*) mice expressing wild-type PrP at even higher levels remain healthy and have a normal lifespan.[12] Of the nine hemizygous Tg(*PG14*) mice used in this study, four were mildly symptomatic at the time of analysis (246 to 264 days of age), and five were terminally ill (361 to 394 days of age) (Table 1). Tg(*PG14*) mice of both the A2 and A3 lines were analyzed with similar results.

Light Microscopy

Light microscopy of both paraffin- and plastic-embedded tissues showed histological lesions and patterns of *PG14*

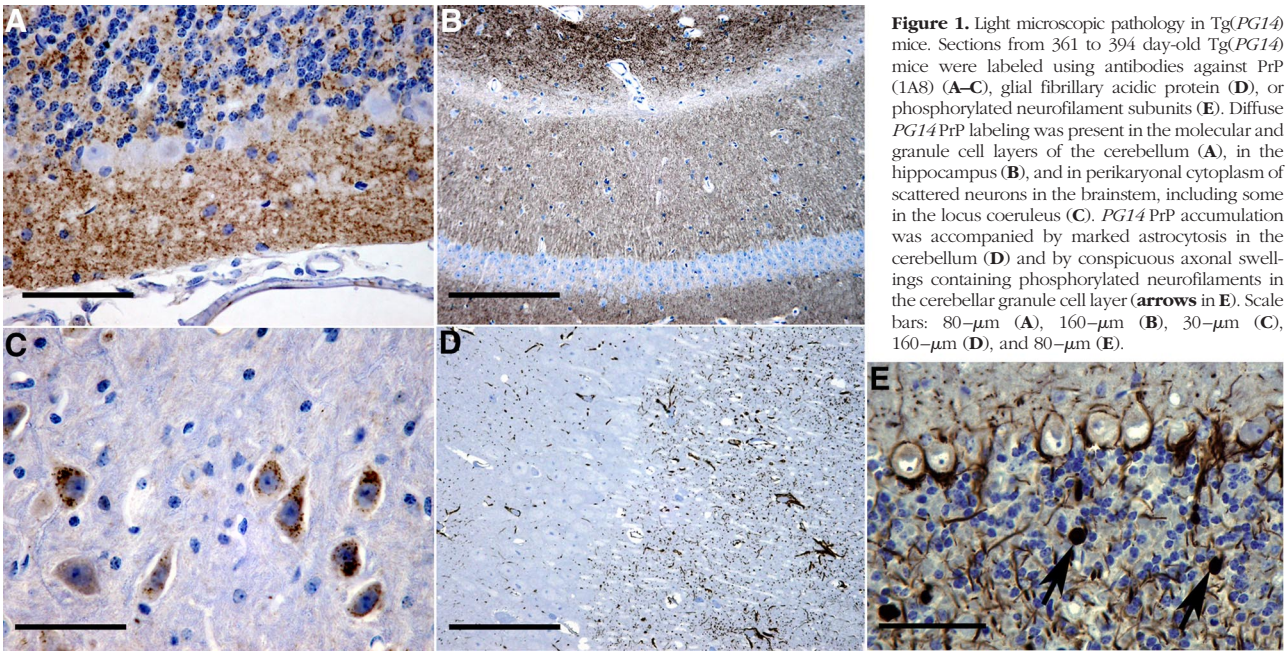

Figure 1. Light microscopic pathology in Tg(*PG14*) mice. Sections from 361 to 394 day-old Tg(*PG14*) mice were labeled using antibodies against PrP (1A8) (**A–C**), glial fibrillary acidic protein (**D**), or phosphorylated neurofilament subunits (**E**). Diffuse *PG14* PrP labeling was present in the molecular and granule cell layers of the cerebellum (**A**), in the hippocampus (**B**), and in perikaryonal cytoplasm of scattered neurons in the brainstem, including some in the locus coeruleus (**C**). *PG14* PrP accumulation was accompanied by marked astrocytosis in the cerebellum (**D**) and by conspicuous axonal swellings containing phosphorylated neurofilaments in the cerebellar granule cell layer (**arrows** in **E**). Scale bars: 80–μm (**A**), 160–μm (**B**), 30–μm (**C**), 160–μm (**D**), and 80–μm (**E**).

PrP labeling similar to those previously reported.[12,14] The cerebellum showed marked granule cell loss and thinning of the molecular layer (Figure 1A). Diffuse *PG14* PrP accumulation was present in the molecular and granule cell layers of the cerebellum (Figure 1A) and throughout the hippocampus, particularly in the stratum lacunosum (Figure 1B). These diffuse *PG14* PrP accumulations were labeled with the 1A8 antibody that recognizes epitopes throughout the PrP molecule (Figure 1, A and B), as well as with the R24 antibody that is directed against an extreme N-terminal epitope (not shown), suggesting that the deposits are composed of N-terminally intact protein. Intense labeling was found in some brainstem neuronal perikarya, such as those in the locus coeruleus (Figure 1C). These intracellular deposits were labeled with antibody 1A8 (Figure 1C), but not antibody R24 (not shown), indicating that they contain N-terminally truncated protein.

Increased astrocytosis was evident with glial fibrillary acidic protein labeling (Figure 1D). Phosphorylated neurofilament labeling showed axonal swellings in the granule cell layer of the cerebellum (Figure 1E). These swellings were frequent in terminally ill mice, and were less frequent in mildly symptomatic mice.

Tg(*WT*) mice did not show any histological abnormalities or PrP labeling at the light microscopic level (not shown).

Subcellular Localization of PG14 PrP by Immunogold Labeling

Our experiments used a postembedding immunogold staining technique[8,9] that does not reveal any labeling of PrP^{C} in Tg(*WT*) or non-transgenic control mice (not shown), presumably reflecting low levels of reactivity of the wild-type protein under these conditions. In addition, there was no labeling of either Tg(*WT*) or Tg(*PG14*) brains with control, pre-immune serum (not shown). Tg(*WT*) control mice did not show any significant ultrastructural lesions (Table 2).

In contrast, specific labeling for *PG14* PrP was observed in both the hippocampus and cerebellum, and was associated with membranes of both dendrites and unmyelinated axons. Labeling was more intense and was more frequently associated with structural abnormalities of the underlying dendritic and axonal processes in terminally ill mice than in mildly symptomatic mice (Table 2).

PG14 PrP was found on the plasma membranes of dendrites at various levels of intensity (Figure 2). Weak and widely dispersed labeling was not associated with detectable morphological changes in the associated dendrites. In areas where light microscopy showed more intense *PG14* PrP accumulation, electron microscopy revealed focal or segmental linear accumulations of gold particles along dendritic plasma membranes (Figure 2, A and B). Some of these intense areas of *PG14* PrP accumulation were associated with irregularity of neurite profiles, and separation of neurites by thin strands of astrocytic or microglial cytoplasm (Figure 2, C–E). Degenerating dendrites occurred throughout the cerebellum and hippocampus, and these were consistently associated with marked *PG14* PrP accumulation (Figure 3, A–D).

PG14 PrP labeling was also observed on membranes of axons, mostly those that were of small diameter and unmyelinated. Labeling was present on axonal shafts, on pre-terminal segments, and on or near axonal boutons. No specific labeling was identified on or adjacent to the axonal pre-synaptic density. Similar to the *PG14* PrP labeling found on dendrites, the labeling on axons occurred as single immunogold foci or as dense immunogold deposits along linear segments of membrane (Figure 4, A–D). In some cases, axonal labeling occurred

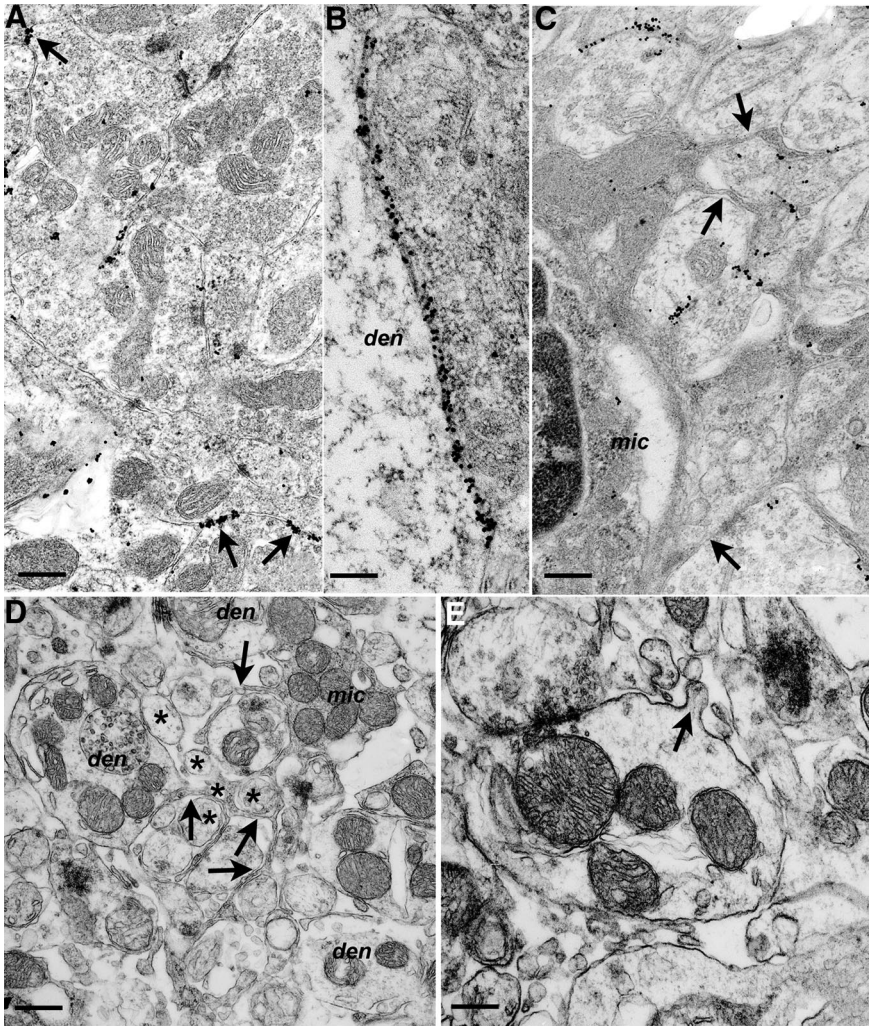

Figure 2. Morphological changes in dendrites and glia associated with membrane labeling for *PG14* PrP. Sections from Tg (*PG14*) mice at 361 to 394 days of age were examined by electron microscopy. **A:** Cerebellar granule cell layer showing individual puncta of *PG14* PrP labeling, as well as short continuous segments of labeling (**arrows**) on the plasmalemmae of adjacent dendrites. **B:** Continuous labeling along a pyramidal neuron dendrite (den) and an adjacent unidentified dendrite from the stratum radiatum of the hippocampus. **C:** *PG14* PrP labeling of dendrites is associated with an activated microglial cell (mic) and strands of microglial cytoplasm (**arrows**) invading between and around labeled processes. **D:** Unlabeled section from the cerebellar molecular layer showing thin strands of cytoplasm (**arrows**) from a microglial cell (mic) enveloping dendrites (den) and parallel fibers (**asterisks**). Parallel fiber axons show atrophy and excessive variation in cross-sectional profiles. **E:** Dendrite from an unlabeled section with an irregular, corrugated profile, part of which has a small outfolding of the plasmalemma (**arrow**). The dendrite is surrounded by excess extracellular space and fragments of tangentially sectioned processes. Scale bars: 0.3–μm (**A**), 0.15–μm (**B**), 0.3–μm (**C**), 0.45–μm (**D**), and 0.3–μm (**E**).

in the absence of any abnormalities of axonal structure, but morphological changes in axons were seen in other labeled areas. We observed a reduction in the density of parallel fibers (granule cell axons) in the molecular layer of the cerebellum, which correlates with the marked thinning of the molecular layer seen by light microscopy in terminally ill mice (Figure 1A; see also[22]). Thinning of the molecular layer was associated with increased contour irregularity, and shrinkage or atrophy of parallel fiber axons (Figure 2D), accompanied by increased extracellular spaces and/or excess interweaving of glial processes. However, no frank degeneration of parallel fiber axons was observed. Despite prominent *PG14* PrP labeling along the membranes of small diameter axons in several brain regions, degenerative changes were observed only in some mossy fiber terminals of the cerebellar granule cell layer, but not elsewhere. However, mossy fiber degeneration is probably not specific to Tg(*PG14*) mice, since it was also rarely observed in Tg(*WT*) animals.

It was not always possible to determine the precise cellular origin of processes showing membrane-associated *PG14* PrP labeling. However, where labeling was light, and the silver-enhanced immunogold accumulations were small (10 to 15–nm diameter), *PG14* PrP could often be localized to individual membranes. Much of the light dendritic labeling was in this form. Even when silver-enhanced immunogold deposits had a larger diameter (>20–nm) and spanned membranes of adjacent processes, labeling could be confidently ascribed to dendrites when each opposing membrane belonged to a dendritic profile (Figure 2A). Similarly, labeling was found on axo-axonal (Figure 4, A–C) and axo-dendritic (Figure 4D) contacts, as well as on axo-somatic and axo-glial contacts (not shown), suggesting that axonal membranes are another source of the linear accumulations of *PG14* PrP. In situations where linear segments of labeling were observed over adjacent axonal and dendritic membranes, these often appeared as parallel lines (Figure 2B), with one line of label on each membrane.

The distribution of immunogold particles spanning pairs of adjacent membranes suggested the possibility that *PG14* PrP aggregates could be transferred between adjacent cells, as has been shown to be the case for infectious PrP^d. For example, PrP^d appears to be transferred from astrocytes to neurons in transgenic mice that express PrP selectively in astrocytes.[20] One suggested mechanism for cell-to-cell transfer of PrP^d involves exo-

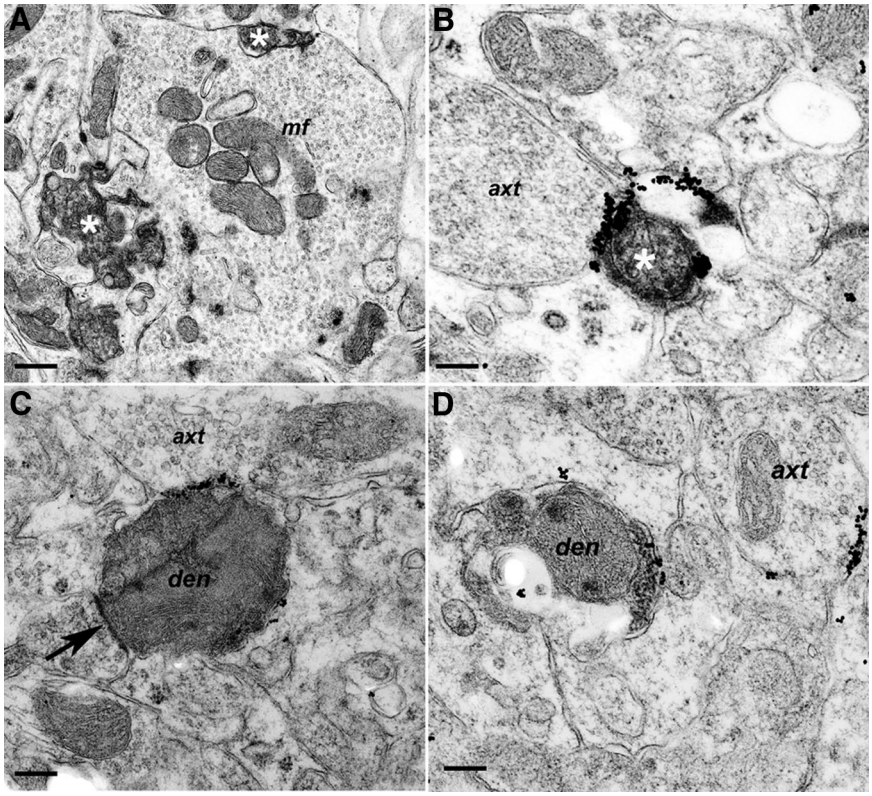

Figure 3. Dendrite degeneration associated with *PG14* PrP labeling. Sections were from Tg (*PG14*) mice at 365 (**A**), 361 (**B**), 264 (**C**), or 361 (**D**) days of age. **A:** Two degenerate dendrites (**asterisks**), defined by their contacts with a mossy fiber terminal (mf), are shown in the granule cell layer of the cerebellum. **B:** A degenerate dendritic process (**asterisk**) in the cerebellar molecular layer showing marked PG14 PrP accumulation at its periphery. The process is in contact with an axon terminal (axt). **C:** Degenerate dendrite (den), as defined by the presence of an in-contact pre-synaptic density (**arrow**), with intense, focal, linear labeling on another pre-terminal axon (axt). **D:** An early-stage degenerating dendrite (den) with sparse membrane accumulation of PG14 PrP is shown. Nearby is an apparently healthy pre-terminal axon (axt), also with membrane PG14 PrP accumulation. Scale bars: 0.45–μm (**A**), 0.15–μm (**B**), 0.25–μm (**C**), and 0.20–μm (**D**).

somes.[23] However, no exosomal structures were seen in the present study. In sheep scrapie, it has been proposed that a protein complex involving PrP^d, a membrane spanning ligand, and ubiquitin is transferred from one membrane to an adjacent one.[9] However, we did not observe co-localization of *PG14* PrP deposits with ubiquitin by immunogold labeling, and in both Tg(PG14) and Tg(*WT*) mice ubiquitin, labeling was confined to a mi-

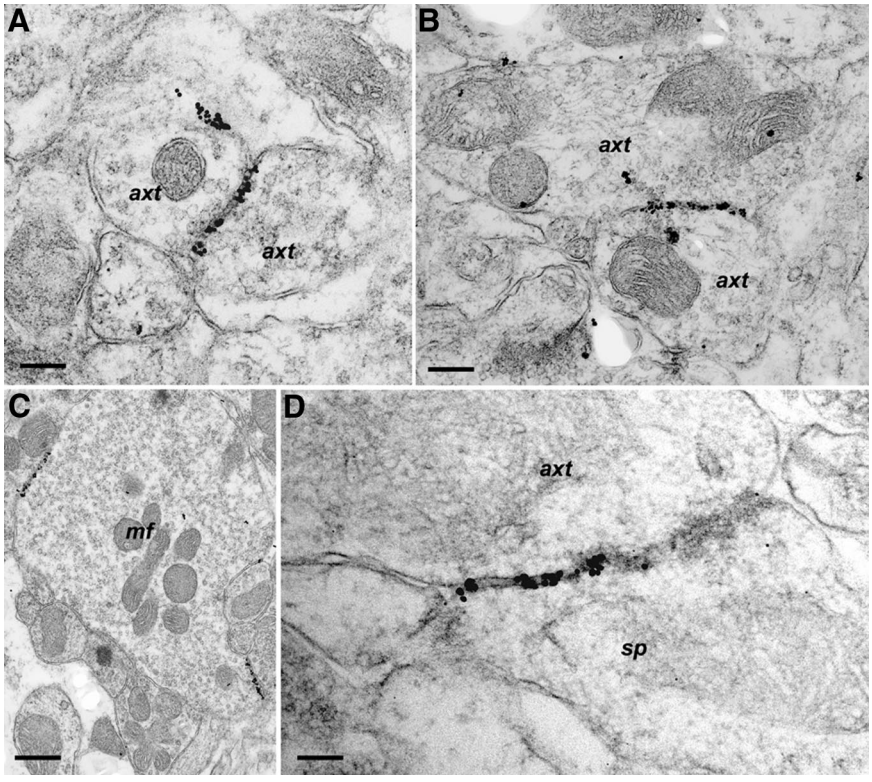

Figure 4. Axon-associated *PG14* PrP labeling. Sections were from Tg (*PG14*) mice at 267 (**A** and **B**), 361 (**C**), or 394 (**D**) days of age. **A:** Labeling of the plasmalemma of processes in the molecular layer of the cerebellum. The labeling lies on membranes of two adjacent axon terminals (axt). **B:** Labeling of membranes of two adjacent axon terminals (axt) in the hippocampus. **C:** Axonal membrane labeling at two points of contact on a mossy fiber terminal (mf) in the granule cell layer of the cerebellum. **D:** Labeling on membranes in the stratum radiatum of the hippocampus. The labeling is on an axon terminal (axt) and a dendritic spine (sp). Scale bars: 0.15–μm (**A**), 0.25–μm (**B**), 0.5–μm (**C**), and 0.1–μm (**D**).

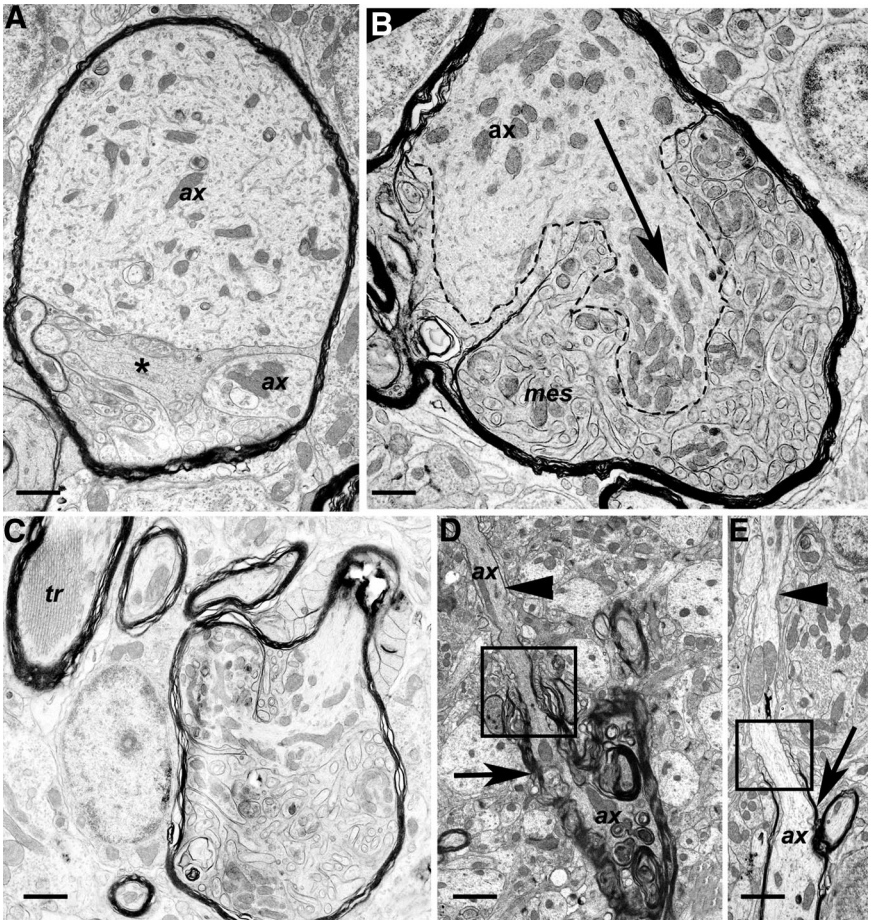

Figure 5. Pathology of myelinated axons and oligodendrocytes. Sections were from Tg (*PG14*) mice at 361 to 365 days of age. **A:** A swollen, myelinated axon divided into two parts (each labeled ax), the topmost of which contains large amounts of fine, fibrillar material, as well as endoplasmic reticulum and mitochondria. Mesaxonal proliferation is also present (**asterisk**). **B:** Axon (ax) showing marked proliferation or sprouting. One clearly defined sprout is indicated by the dashed lines and **arrow**. Prominent and highly complex proliferation of the inner mesaxon (mes) is also present, but the small size of the oligodendroglial and axonal sprouts makes it difficult to reliably distinguish between processes. **C:** A swollen myelinated axon with proliferation of the oligodendroglial, mesaxonal cytoplasm, and invasion of the axonal cytoplasm with partial compartmentalization by myelin. A myelinated process with a tubulo-reticular inclusion (tr) is adjacent. **D:** A degenerate myelinated process shows marked variation in myelin thickness. A thick myelin sheath is present on the lower part of the axon (**arrow**), with thin myelin on the upper part (**arrowhead**) above the paranode (**square**). The lower part of the axon is undergoing degeneration. ax; axon. **E:** An extended section of bare, unmyelinated axon (**arrowhead**) appears above the paranode (**square**) of a myelinated axon (**arrow**). ax, axon. Scale bars: 1.15–μm (**A**), 0.9–μm (**B**), 1.2–μm (**C**), 1.6–μm (**D**), and 1.6–μm (**E**).

nority of multivesicular bodies and lysosomes (not shown).

We only rarely observed immunogold labeling for *PG14* PrP over organelles of the secretory or endocytic pathways in neuronal cell bodies (not shown). On three neurons in both hippocampus and cerebellum, small foci of *PG14* PrP accumulation were found in the endoplasmic reticulum. Intralysosomal *PG14* PrP accumulation was occasionally observed in neurons of the hippocampus and cerebellar granule cell layer, and in astrocytes and microglial cells. Lysosomal labeling was more frequent in neurons of the locus coeruleus, corresponding to the intense intracellular labeling seen by light microscopy (Figure 1C). These neurons appeared morphologically normal.

In agreement with light microscopic and DNA laddering studies,[14,22] apoptotic neurons were commonly identified by electron microscopy in the cerebellum of Tg(*PG14*) mice, and were occasionally found in the hippocampus. None of the apoptotic neuronal cell bodies were associated with *PG14* PrP labeling (not shown).

Pathology of Myelinated Axons in Tg(PG14) Mice

One striking feature observed in our electron microscopic analysis, which had not been appreciated in previous light microscopic studies, was the presence of abnormalities in myelinated axons. These abnormalities were seen primarily in single myelinated processes as they traversed gray matter, most conspicuously in the granule cell layer of the cerebellum. Axons in major white matter tracts (in the cerebellum or corpus callosum, for example) were generally not affected. Axonal pathology was of greater severity in older mice (Table 2). Notably, none of the axonal inclusions or lesions of myelinated axons described below showed any immunogold labeling for *PG14* PrP.

One type of axonal lesion consisted initially of an increase in diameter and organelle content, leading progressively to markedly swollen axons, often adjacent to nodes of Ranvier or paranodal segments. Swollen axons were packed with ~8- to 10-nm diameter filaments, and varying amounts of endoplasmic reticulum and mitochondria (Figure 5A). Based on their frequency and distribution, the swollen axons observed by electron microscopy likely correspond to those identified by light microscopy using antibodies to phosphorylated neurofilament subunits (Figure 1E). The individual filaments within the swollen axons had a diameter consistent with their identification as neurofilaments.

Another lesion of myelinated processes consisted of a proliferation of the inner mesaxons, which represent the inner tongues of oligodendroglial cytoplasm in a myelin-

ated axon (Figure 5, A–C). Some of these lesions displayed a highly complex pattern characterized by many small axonal sprouts (Figure 5B) and invasion of the axoplasm by the oligodendrocyte mesaxons. Sometimes both axonal inclusions and axonal-oligodendrocyte pathology occurred in the same myelinated process (Figure 5A).

Other abnormalities of myelinated axons included Wallerian-type degeneration (suggesting loss of axons), excessively thick myelin (suggesting axonal atrophy), and tubulo-reticular inclusions (Figure 5C). We also observed increased nodal gaps and unmyelinated (Figure 5D) or poorly myelinated segments (Figure 5E), suggestive of an ongoing repair process.

Discussion

This study is the first ultrastructural analysis of the brains of Tg(*PG14*) mice, which model key features of familial prion diseases in humans. Our results reveal prominent accumulations of *PG14* PrP along both axonal and dendritic membranes. In addition, we describe specific ultrastructural lesions of both axons and dendrites. Our results suggest cellular mechanisms by which mutant prion proteins produce pathology, and they allow a detailed comparison of the subcellular pathology of familial and infectious prion diseases.

Cellular Localization and Trafficking of PG14 PrP

Previous light microscopic immunohistochemical studies of Tg(*PG14*) mice identified diffuse punctate deposits of *PG14* PrP in the cerebellar cortex, and gray matter of the hippocampus and neocortex.[12,14] These deposits were characterized as "synaptic-like," since they had a distribution reminiscent of synaptic terminals. However, their subcellular localization was unknown. The results presented here demonstrate that *PG14* PrP accumulates on the plasma membranes of dendrites and axons. Although in some cases *PG14* PrP was found on pre-terminal axonal membranes, it was never associated with pre- or post-synaptic densities. Thus, the accumulations are not truly synaptic in their localization.

Previous studies have shown that PrP^C is trafficked along secretory pathways and distributed to the cell surface, where it is attached by its glycosylphosphatidylinositol anchor.[24] At steady state, PrP^C is localized primarily on the plasma membrane and in the Golgi apparatus of cultured cells.[25] PrP^C is expressed on axons of mature hippocampal neurons in culture[26] and embryonic retinal ganglion cells in explants,[27] and has been visualized on both dendrites and axons by cryo-electron microscopy of brain tissue.[28] In the brains of transgenic mice expressing an *EGFP*-tagged version of wild-type PrP, the fusion protein is localized primarily on axons and presynaptic terminals, and is excluded from cell bodies and dendrites.[29]

Some aspects of the cellular distribution and trafficking of mutant forms of PrP differ from those of wild-type PrP^C. Mutant PrPs, including *PG14* PrP, are partially retained in the endoplasmic reticulum of cultured cells, and are inefficiently delivered to the cell surface concomitant with a delay in the oligosaccharide processing of these molecules.[25,30,31] Pulse-chase labeling experiments indicate that conformational alteration of *PG14* PrP molecules is a step-wise process that begins soon after synthesis in the endoplasmic reticulum, with the protein becoming gradually more aggregated and protease-resistant with time.[32] These molecular alterations likely contribute to impaired movement of mutant PrP through the secretory pathway.

In contrast to these studies of cultured cells, in the present investigation we only rarely observed immunogold-labeled deposits of *PG14* PrP in neuronal perikarya associated with organelles of the secretory pathway. This discrepancy probably reflects the lability of monomeric or small aggregates of *PG14* PrP found in these intracellular sites to the postembedding labeling technique used for electron microscopy. It is possible that, once *PG14* PrP reaches the plasma membrane, it accumulates as larger aggregates or is otherwise stabilized as a multimolecular membrane complex that can be visualized by electron microscopy. Intracellular *PG14* PrP labeling was found in lysosomes of some neurons in the locus coeruleus. At these sites, *PG14* PrP was N-terminally truncated, consistent with internalization from the cell surface and subsequent processing by lysosomal proteases.

Recently, we characterized the localization of *PG14* PrP in brains of Tg(*PG14-EGFP*) mice expressing a fusion of the mutant protein to enhanced green fluorescent protein.[15] Aggregates of the *PG14* PrP-*EFGP* were prominent in myelinated and unmyelinated axonal tracts in brain and peripheral nerve of these mice, and similar deposits were seen in the processes of cultured neurons expressing the fusion protein. In contrast, in the present study *PG14* PrP was not observed within axons, but was seen on plasma membranes of single, unmyelinated but not myelinated axons. The absence of intra-axonal *PG14* PrP in ultrastructural studies may be due to the loss of intracellular *PG14* PrP during tissue preparation, although artifactual effects of the *EGFP* tag, or the relatively low expression level of the fusion protein in Tg(*PG14-EGFP*) mice may also be factors.

Significance of Axonal/Oligodendroglial Pathology

A major form of pathology that was not appreciated in previous light microscopic analyses of Tg(*PG14*) mice involves abnormalities in myelinated axons and axon-oligodendrocyte interactions, which begin in the early symptomatic phase. Several of these abnormalities are suggestive of impaired axonal transport, in particular axonal swellings, filamentous inclusions, nodal increases in organelle content, and Wallerian-type axonal degeneration. Thus, the axonal pathology described here is consistent with our proposal, based on analysis of Tg(*PG14-EGFP*) mice,[15] that *PG14* and other aggregation-prone PrP molecules could induce pathology by blocking or altering normal axonal transport processes.

We also observed lesions suggestive of dysregulation of axonal-oligodendrocyte interactions, including segmental variation in myelination, invasion of axoplasm by oligodendrocyte processes, and a distinctive proliferation of inner-tongue, oligodendroglial cytoplasm (mesaxonal proliferation). It is possible that these abnormalities reflect reaction of the oligodendrocyte to the presence of intra-axonal *PG14* PrP aggregates or other toxic inclusions, analogous to a mechanism that has been proposed for toxic leukoencephalopathies.[33]

Mesaxon proliferation has been described in the optic nerves of a rodent model of infectious prion disease.[34] In this model, however, mesaxonal changes are subtle, and may be a nonspecific component of widespread white matter tract degeneration common to panencephalic forms of rodent prion disease. In addition, mesaxonal proliferation in rodent models of infectious prion disease is not accompanied by other changes such as axonal sprouting or inclusions found in the Tg(*PG14*) mouse. Thus, we consider the white matter pathology induced by the *PG14* mutation to be unique.

Strikingly, none of these lesions of myelinated axons is associated with immunogold-labeling for *PG14* PrP. However, if *PG14* PrP is subject to rapid anterograde or retrograde axonal transport, it might be present only transiently or at low levels at any particular point along the course of the axon. Moreover, the protein may undergo degradation as part of the neurodegenerative process.

Other Neurotoxic Mechanisms

Besides axon-oligodendrocyte lesions, our results show degenerative changes in dendrites that colocalize with plasma membrane deposits of *PG14* PrP. We also observed lesions of unmyelinated axons that were associated with labeling for *PG14* PrP, including atrophy and irregularity of axonal contours. These results suggest that accumulations of *PG14* PrP may be directly toxic to axons and dendrites, perhaps by physically damaging the structure of the plasma membrane, or by activating pathological signaling pathways. Both dendritic and axonal changes may also be secondary to interaction with glia, a possibility suggested by our observation that *PG14* PrP-labeled dendrites and unmyelinated axons were often enveloped by glial processes. *PG14* PrP at the plasma membrane could elicit glial envelopment, thereby removing synaptic contacts, and resulting in loss of anterograde or retrograde signals. Finally, aggregates of the mutant protein may interact with other membrane constituents to alter physiological function in the absence of morphological change.

Apoptotic granule neurons in the cerebellum were not labeled for *PG14* PrP although degenerated dendrites and neurites ensheathed by glial cells were labeled. Potentially, damage to granule cell neurites may lead to apoptosis in the absence of perikaryonal *PG14* PrP labeling. Deletion of the pro-apoptotic protein, Bax, from Tg(*PG14*) mice preserves granule neuron cell bodies, but fails to prevent shrinkage of the molecular layer or clinical disease.[22] Thus, neurological deficits correlate with loss of neuronal processes rather than cell bodies. The morphological changes in axons and dendrites we have described here are consistent with this proposal. We did not observe acutely degenerating parallel fibers in the molecular layer that would correspond to axons of apoptotic granule neurons, most likely because such fibers undergo involution and retraction rather than frank degeneration.

Comparison with Infectious Prion Diseases

The present study highlights several differences between the lesions seen in Tg(*PG14*) mice and those present in infectious prion diseases (Table 2). Distinctive morphological features of infectious prion diseases that are absent from Tg(*PG14*) mice include vacuolation, tubulovesicular bodies, and several morphological changes of plasma membranes such as abnormal spiral invaginations and presence of excess ubiquitin.[9,20] Conversely, the axon-oligodendrocyte abnormalities seen in Tg(*PG14*) mice are absent in the infectious prion diseases.[8,11]

There are also notable differences between *PG14* PrP and PrP^d in their localization and associated morphological changes. Previous studies of infectious prion disease show that PrP^d accumulates primarily on neuronal perikaryonal and dendritic plasma membranes, with little specific accumulation on axons.[8,9,11] In contrast, *PG14* PrP is present on both axonal and dendritic plasma membranes, but not on perikarya. Additionally, PrP^d in infectious prion diseases is distributed uniformly on plasma membranes and is colocalized with ubiquitin, abnormal endocytosis, and membrane microfolding. In contrast, *PG14* PrP accumulations often occupy a continuous length of membrane, do not colocalize with ubiquitin, and do not elicit abnormal endocytosis or microfolding. Finally, Tg(*PG14*) mice show frank necrosis of dendrites but not axons, while the reverse is true in rodent scrapie.[11]

These distinctions between the pathology seen in Tg(*PG14*) mice and in infectious prion disease likely reflect differences between *PG14* PrP and PrP^d in cellular localization, trafficking, and metabolism. PrP^C is located primarily on the plasma membrane, and during prion infection undergoes conversion to its abnormal counterpart on the cell surface or following internalization into endosomes.[35,36] In contrast, *PG14* PrP undergoes conformational alterations in the secretory pathway, and as a consequence is not delivered efficiently to the plasma membrane.[25,30,32] In neurons, *PG14-EGFP* is exported into axons, where it forms intracellular aggregates.[15] Thus, differential involvement of secretory versus endocytic pathways in the trafficking of *PG14* PrP and PrP^d, respectively, may explain differences in the localization of the two kinds of abnormal protein.

Even though it is not transmissible, *PG14* PrP shares several key biochemical properties with PrP^d.[13] These include aggregation propensity, protease resistance, patterns of epitope exposure, and binding to metal ions and phosphotungstate. Thus, although *PG14* PrP and PrP^d display different distribution profiles at the ultra-

structural level, at least some of the molecular mechanisms underlying their pathogenicity may be similar. To test this possibility, it will be necessary to understand more about the cellular signaling pathways underlying the neurotoxicity of both mutant and infectious forms of PrP.

Acknowledgments

We are grateful to Byron Caughey for the R24 antibody. We also acknowledge Cheryl Adles and Su Deng for mouse colony maintenance and genotyping.

References

1. Prusiner SB: An introduction to prion biology and diseases. Prion Biology and Diseases. Edited by Prusiner SB. Cold Spring Harbor, New York, Cold Spring Harbor Laboratory Press, 2004, pp 1–66
2. Aguzzi A, Sigurdson C, Heikenwalder M: Molecular mechanisms of prion pathogenesis. Annu Rev Pathol 2008, 3:11–40
3. Prusiner SB: Prions. Proc Natl Acad Sci USA 1998, 95:13363–13383
4. Chiesa R, Harris DA: Prion diseases: what is the neurotoxic molecule? Neurobiol Dis 2001, 8:743–763
5. Chiesa R, Piccardo P, Quaglio E, Drisaldi B, Si-Hoe SL, Takao M, Ghetti B, Harris DA: Molecular distinction between pathogenic and infectious properties of the prion protein. J Virol 2003, 77:7611–7622
6. Piccardo P, Manson JC, King D, Ghetti B, Barron RM: Accumulation of prion protein in the brain that is not associated with transmissible disease. Proc Natl Acad Sci USA 2007, 104:4712–4717
7. Gonzalez L, Terry L, Jeffrey M: Expression of prion protein in the gut of mice infected orally with the 301V murine strain of the bovine spongiform encephalopathy agent. J Comp Pathol 2005, 132: 273–282
8. Jeffrey M, Goodsir CM, Bruce M, McBride PA, Scott JR, Halliday WG: Correlative light and electron microscopy studies of PrP localisation in 87V scrapie. Brain Research 1994, 656:329–343
9. Jeffrey M, McGovern G, Goodsir CM, Siso S, Gonzalez L: Strain associated variations in abnormal PrP trafficking of sheep scrapie. Brain Pathol 2009, 19:1–11
10. Ersdal C, Goodsir CM, Simmons MM, McGovern G, Jeffrey M: Abnormal prion protein is associated with changes of plasma membranes and endocytosis in BSE-affected cattle brains. Neuropathol Appl Neurobiol 2009, 35:259–271
11. Jeffrey M, Halliday WG, Bell J, Johnston AR, MacLeod NK, Ingham C, Sayers AR, Brown DA, Fraser JR: Synapse loss associated with abnormal PrP precedes neuronal degeneration in the scrapie-infected murine hippocampus. Neuropathol Appl Neurobiol 2000, 26:41–54
12. Chiesa R, Piccardo P, Ghetti B, Harris DA: Neurological illness in transgenic mice expressing a prion protein with an insertional mutation. Neuron 1998, 21:1339–1351
13. Biasini E, Medrano AZ, Thellung S, Chiesa R, Harris DA: Multiple biochemical similarities between infectious and non-infectious aggregates of a prion protein carrying an octapeptide insertion. J Neurochem 2008, 104:1293–1308
14. Chiesa R, Drisaldi B, Quaglio E, Migheli A, Piccardo P, Ghetti B, Harris DA: Accumulation of protease-resistant prion protein (PrP) and apoptosis of cerebellar granule cells in transgenic mice expressing a PrP insertional mutation. Proc Natl Acad Sci USA 2000, 97:5574–5579,
15. Medrano AZ, Barmada S, Biasini E, Harris DA: GFP-tagged mutant prion protein forms intra-axonal aggregates in transgenic mice. Neurobiol Dis 2008, 31:20–32
16. Farquhar CF, Somerville RA, Ritchie LA: Post-mortem immunodiagnosis of scrapie and bovine spongiform encephalopathy. J Virol Methods 1989, 24:215–222
17. Caughey B, Raymond GJ, Ernst D, Race RE: N-Terminal truncation of the scrapie-associated form of PrP by lysosomal protease (s): Implications regarding the site of conversion of PrP to the protease-resistant state. J Virol 1991, 65:6597–6603
18. Korth C, Stierli B, Streit P, Moser M, Schaller O, Fischer R, Schulz-Schaeffer W, Kretzschmar H, Raeber A, Braun U, Ehrensperger F, Hornemann S, Glockshuber R, Riek R, Billeter M, Wüthrich K, Oesch B: Prion (PrP^{Sc})-specific epitope defined by a monoclonal antibody. Nature 1997, 390:74–77
19. Bolton DC, Seligman SJ, Bablanian G, Windsor D, Scala LJ, Kim KS, Chen CM, Kascsak RJ, Bendheim PE: Molecular location of a species-specific epitope on the hamster scrapie agent protein. J Virol 1991, 65:3667–3675
20. Jeffrey M, Goodsir CM, Race RE, Chesebro B: Scrapie-specific neuronal lesions are independent of neuronal PrP expression. Ann Neurol 2004, 55:781–792
21. Jeffrey M, Goodsir CM, Bruce ME, McBride PA, Fraser JR: In vivo toxicity on prion protein in murine scrapie: ultrastructural and immunogold studies. Neuropath Appl Neurobiol 1997, 23:93–101
22. Chiesa R, Piccardo P, Dossena S, Nowoslawski L, Roth KA, Ghetti B, Harris DA: Bax deletion prevents neuronal loss but not neurological symptoms in a transgenic model of inherited prion disease. Proc Natl Acad Sci USA 2005, 102:238–243
23. Fevrier B, Vilette D, Archer F, Loew D, Faigle W, Vidal M, Laude H, Raposo G: Cells release prions in association with exosomes. Proc Nat Acad Sci USA 2004, 101:9683–9688
24. Harris DA: Trafficking, turnover and membrane topology of PrP. Br Med Bull 2003, 66:71–85
25. Ivanova L, Barmada S, Kummer T, Harris DA: Mutant prion proteins are partially retained in the endoplasmic reticulum. J Biol Chem 2001, 276:42409–42421
26. Galvan C, Camoletto PG, Dotti CG, Aguzzi A, Ledesma MD: Proper axonal distribution of PrP^{C} depends on cholesterol-sphingomyelin-enriched membrane domains and is developmentally regulated in hippocampal neurons. Mol Cell Neurosci 2005, 30:304–315
27. Sales N, Hassig R, Rodolfo K, DiGiamberardino L, Traiffort E, Ruat M, Fretier P, Moya KL: Developmental expression of the cellular prion protein in elongating axons. Eur J Neurosci 2002, 15:1163–1177
28. Mironov A, Latawiec D, Wille H, Bouzamondo-Bernstein E, Legname G, Williamson RA, Burton D, DeArmond SJ, Prusiner SB, Peters PJ: Cytosolic prion protein in neurons. J Neurosci 2003, 23:7183–7193
29. Barmada S, Piccardo P, Yamaguchi K, Ghetti B, Harris DA: GFP-tagged protein is correctly localised and functionally active in the brains of transgenic mice. Neurobiol Dis 2005, 16:527–537
30. Drisaldi B, Stewart RS, Adles C, Stewart LR, Quaglio E, Biasini E, Fioriti L, Chiesa R, Harris DA: Mutant PrP is delayed in its exit from the endoplasmic reticulum, but neither wild-type nor mutant PrP undergoes retrotranslocation prior to proteasomal degradation. J Biol Chem 2003, 278:21732–21743
31. Fioriti L, Dossena S, Stewart LR, Stewart RS, Harris DA, Forloni G, Chiesa R: Cytosolic prion protein (PrP) is not toxic an N2Acells and primary neurons expressing pathogenic PrP mutations. J Biol Chem 2005, 280:11320–11328
32. Daude N, Lehmann S, Harris DA: Identification of intermediate steps in the conversion of a mutant prion protein to a scrapie-like form in cultured cells. J Biol Chem 1997, 272:11604–11612
33. Hemm RD, Carlton WW, Welser JR: Ultrastructural changes of cuprizone toxicity in mice. Toxicol Appl Pharmacol 1971, 18:869–882
34. Walis A, Liberski PP: Proliferation of mesaxons in the optic nerve of hamsters infected with the Echigo-1 strain of Creutzfeldt-Jakob disease. Acta Neurobiologiae Experimentalis 1999, 59:177–180
35. Caughey B, Raymond GJ: The scrapie-associated form of PrP is made from a cell surface precursor that is both protease- and phospholipase-sensitive. J Biol Chem 1991, 266:18217–18223
36. Borchelt DR, Taraboulos A, Prusiner SB: Evidence for synthesis of scrapie prion proteins in the endocytic pathway. J Biol Chem 1992, 267:16188–16199